Melting of Saturated Fatty Acid Zinc Soaps

S. Barman[†] and S. Vasudevan*[,†,‡]

Solid State and Structural Chemistry Unit and Department of Inorganic and Physical Chemistry, Indian Institute of Science, Bangalore-566012, India

Received: July 9, 2006; In Final Form: August 19, 2006

The melting of alkyl chains in the saturated fatty acid zinc soaps of different chain lengths, $Zn(C_nH_{2n+1}COO)_2$; $n = 11$, 13, 15, and 17, have been investigated by powder X-ray diffraction, differential scanning calorimetry, and vibrational spectroscopy. These compounds have a layer structure with the alkyl chains arranged as tilted bilayers and with all methylene chains adopting a planar, all-trans conformation at room temperature. The saturated fatty acid zinc soaps exhibit a single reversible melting transition with the associated enthalpy change varying linearly with alkyl chain length, but surprisingly, the melting temperature remaining constant. Melting is associated with changes in the conformation of the alkyl chains and in the nature of coordination of the fatty acid to zinc. By monitoring features in the infrared spectra that are characteristic of the global conformation of the alkyl chains, a quantitative relation between conformational disorder and melting is established. It is found that, irrespective of the alkyl chain length, melting occurs when 30% of the chains in the soap are disordered. These results highlight the universal nature of the melting of saturated fatty acid zinc soaps and provide a simple explanation for the observed phenomena.

Introduction

Structural phase transitions in monolayer and bilayer assemblies of flexible rodlike molecules have been extensively studied. These quasi-two-dimensional systems are ideally suited for the study of reduced dimensionality on physical properties. In addition, the phase transitions in these systems are closely related to phase transitions in biological membranes and smectic liquid crystals. In these systems it is clear that it is the accumulation of gauche defects with temperature that plays a central role in deciding the nature and temperature of the order−disorder transition. Despite numerous studies, however, quantitative information on the relation between molecular conformation and the melting of the assembly has yet to be clearly established. This in part is because many of these systems, especially the lipid bilayers, have the experimental drawback that they are essentially liquidlike and hence not amenable for study by powerful solid-state spectroscopic techniques.

Fatty acids and their metal salts, or soaps, are among the simplest model systems for lipid bilayers.[1] But unlike lipid assemblies that are essential fluidlike most soaps are solids at ambient temperatures. In addition to their role as simple model systems for the more complex lipid membrane assemblies, soaps are also of considerable commercial importance. They find applications in diverse areas that include driers in paints and inks, components of lubricating greases, heat stabilizers for plastics,[2] catalysts, waterproofing agents, fuel additives, and cosmetic products.[3,4] The title compounds were chosen for this study because the zinc fatty acid salts, unlike most other polyvalent metal soaps, are known to pass directly from the solid to liquid phase.[5] Most other soap shows a series of multiple transitions and intermediate meso phases that include solid−solid, solid−liquid crystal, and liquid crystal−liquid crystal transitions. These transitions and phases are known to be influenced by a number of factors that include the nature and extent of hydration of the metal ion.[6−10] In zinc carboxylates, however, the zinc metal ions are not hydrated and only a single transition has been reported from differential scanning calorimetry (DSC) measurements.[5]

We have compared the structure and melting behavior of the zinc salts of saturated fatty acids of varying chain length, $Zn(C_nH_{2n+1}COO)_2$ ($n = 11$, 13, 15, 17), using X-ray diffraction, DSC measurements, and infrared vibrational spectroscopy. Although crystal structures of the longer fatty acid zinc soaps have not been reported, based on X-ray absorption[11] and infrared spectroscopic studies,[12] and from reported structures of Zn soaps with shorter hydrocarbon chains,[13] it is reasonable to conclude that these compounds, too, have a layer structure with tetrahedrally coordinated Zn cations connected by carboxylate bridges in a syn ± anti arrangement with the alkyl chains arranged in a tilted fashion. Here we make use of the progression bands in the infrared spectrum that arise from a coupling of vibrational modes of methylene units in trans registry to monitor the conformation of the alkyl chains. These bands are characteristic of the global conformation of the hydrocarbon chain and can provide a quantitative measure of the concentration of all-trans planar chains in the ensemble and its variation as the temperature approaches that of the melt. We show that there is a critical concentration of conformational disorder at which melting occurs that is the same irrespective of the chain length of the fatty acid. Our results highlight the universal nature of melting in this class of materials.

Experimental Section

The saturated fatty acid zinc soaps were prepared by a metathesis reaction in alcoholic solution that involved two steps. In the first step the sodium salts of the saturated fatty acid were prepared by dissolving the fatty acid, $C_nH_{2n+1}COOH$, $n = 11$, 13, 15, 17 (Aldrich), in hot 95% ethanol and then adding

* To whom correspondence may be addressed. E-mail: svipc@ipc.iisc.ernet.in. Tel: +91-80-2293-2661. Fax: +91-80-2360-1552/0683.
† Solid State and Structural Chemistry Unit.
‡ Department of Inorganic and Physical Chemistry.

10.1021/jp064306p CCC: $33.50
Published on Web 10/19/2006

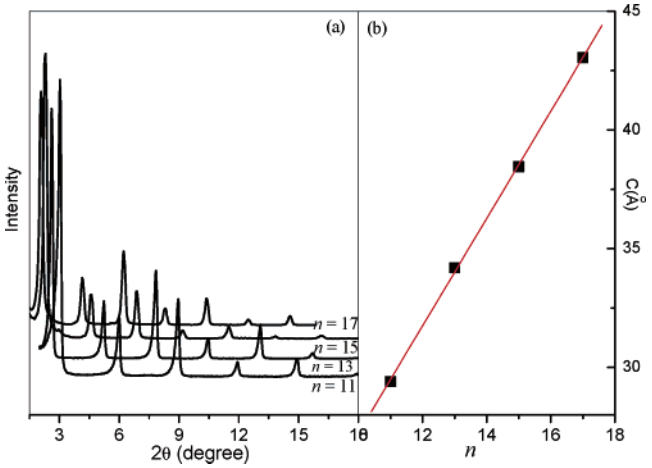

Figure 1. (a) Powder X-ray diffraction patterns of $Zn(C_nH_{2n+1}COO)_2$; $n = 11$, 13, 15, and 17 and (b) the corresponding interlayer spacing vs n.

stoichiometric amounts of solid NaOH to form the corresponding sodium carboxylates. In the second step a stoichiometric quantity of $ZnCl_2$(aq) is added to the alcoholic solution. The resulting precipitate was filtered and washed in ethanol and water.

DSC measurements were recorded on a Perkin-Elmer DSC-2C instrument operated at a scanning rate of 5 K/min under N_2 atmosphere. The temperature scale and enthalpies were calibrated using an indium standard. Powder X-ray diffraction patterns were recorded on a Shimadzu XD-D1 diffractometer using Cu Kα radiation. Variable temperature infrared spectra were recorded on a Perkin-Elmer spectrum 2000 FT-IR spectrometer in the diffuse reflectance mode using a DRIFT (P/N 19900 series) accessory with a cooled MCT detector.

Results

X-ray Diffraction. The X-ray diffraction patterns of the saturated fatty acids zinc soaps of differing chain length, $Zn(C_nH_{2n+1}COO)_2$ ($n = 11$, 13, 15, 17), are shown in Figure 1a. The compounds show a well-developed progression of intense 00*l* Bragg reflections which may be indexed to a unique interlayer spacing. The X-ray patterns indicate the layer nature of the zinc soaps; only 00*l* reflections are observed indicating an extremely high degree of preferred orientation arising as a consequence of the layered morphology of these compounds. The plot of interlayer spacing vs number of carbon atoms in the fatty acids show a linear increase with slope 1.1 (Figure 1b). The values of the interlayer spacing suggest that the structure is formed from zinc carboxylate sheets separated by alkyl chain bilayers. For an all-trans alkyl chain the addition of a methylene unit to the chain increments its length by 1.25 Å. If the alkyl chains in zinc soaps are in all-trans conformation then the slope of Figure 1b indicates that the chains are arranged as a tilted bilayers with the tilt angle, the angle between the interlayer normal and the molecular axis of the alkyl chains is 28° as shown schematically in Figure 2.

Phase Transitions. *DSC Measurements.* The DSC traces of $Zn(C_nH_{2n+1}COO)_2$ ($n = 11$, 13, 15, 17) are shown in Figure 3a. On heating a single endotherm corresponding to a first-order phase transition is observed at 403 K in all four compounds. The transition is reversible. On cooling an exotherm is observed but with considerable hysteresis. This transition corresponds to the melting of the zinc soaps. This was confirmed by variable temperature X-ray diffraction measurements, which showed the complete disappearance of Bragg peaks at the temperature of the DSC endotherm (see Supporting Information). The enthalpy of the melting transition was obtained from the integrated area under the DSC peak and was found to increase linearly as a function of chain length (Figure 3b). The transition temperature and enthalpy changes are given in Table 1. The entropy change per methylene unit across the transition, calculated from the DSC enthalpies, is also given.

A remarkable feature of the melting of the zinc soaps is that although the enthalpy change associated with melting increases linearly with chain length, the transition temperatures are identical, 403 K. This behavior may be contrasted with that of the corresponding fatty acids, $C_nH_{2n+1}COOH$, where both the transition temperature and enthalpy change vary linearly with chain length (Table 1). A common feature of the zinc carboxylates and the fatty acids is that the entropy change per methylene units across the melting transition is independent of chain length and is roughly the same for both classes of compounds. The enthalpy of fusion per methylene unit may be obtained from the slope of Figure 3b. The value of 4.4 KJ (mol of CH_2)$^{-1}$ for the zinc soaps is slightly higher than that reported for crystalline alkanes[14] and the europium alkanoates (3.8 KJ (mol per CH_2)$^{-1}$).[9]

Vibrational Spectroscopy. The infrared spectrum can provide information on both conformation of the alkyl chain and its changes with temperature, as well as the nature of coordination of the fatty acid carboxylic group with zinc. A typical room-temperature spectrum of a saturated fatty acid zinc salt is shown

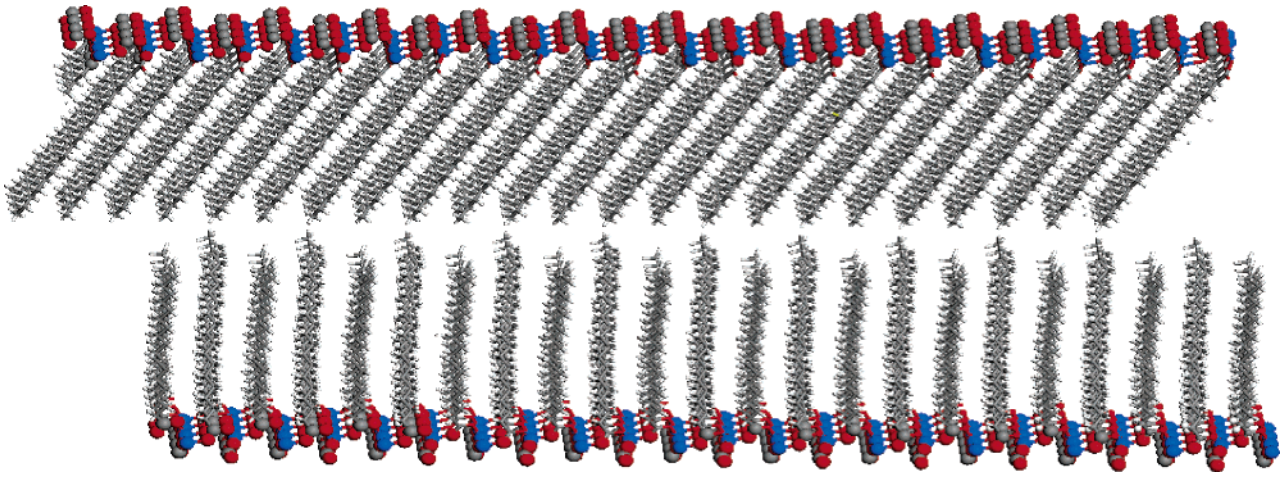

Figure 2. Schematic structure of a saturated fatty acid zinc soap. Blue, Zn; red, O; grey, C; white, H.

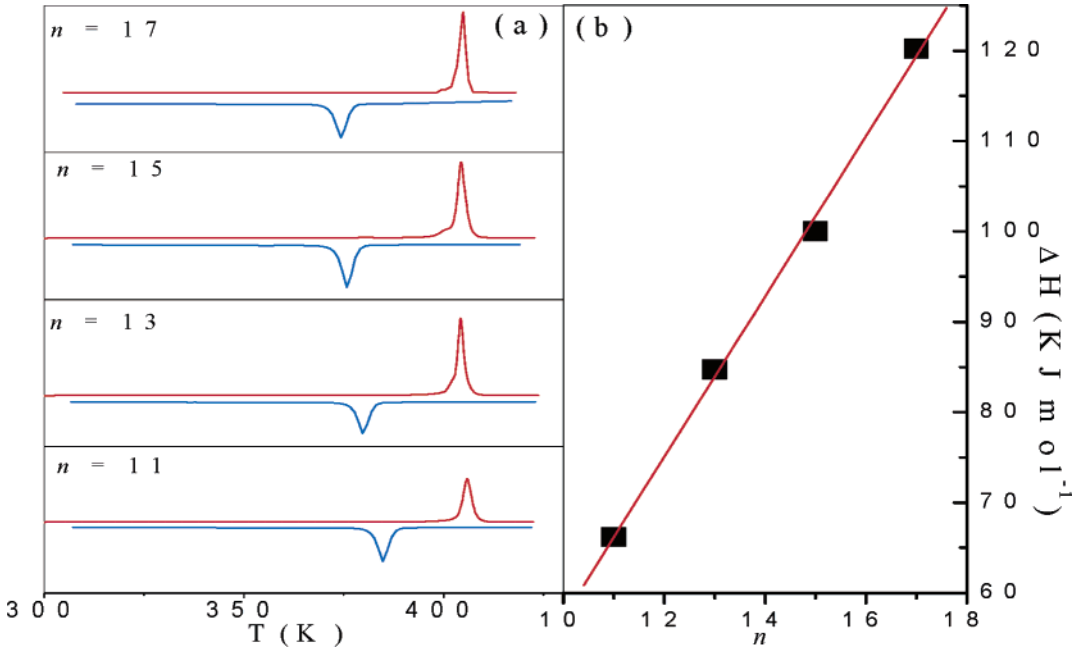

Figure 3. (a) DSC traces of the first heating (red lines) and cooling cycle (blue lines) for $Zn(C_nH_{2n+1}COO)_2Zn$; $n = 11, 13, 15, 17$. (b) Corresponding enthalpy change vs chain length (n).

TABLE 1: Summary of the Transition Enthalpies and Entropies Accompanying the Melting of Zinc Soaps, $Zn(C_nH_{2n+1}COO)_2Zn$ and Fatty Acids

zinc soaps	T_m (K)	ΔH (KJ mol^{-1})	ΔS (JK^{-1} mol^{-1}, per CH_2 unit)	fatty acids	T_m (K)	ΔH (KJ mol^{-1})	ΔS (JK^{-1} mol^{-1}, per CH_2 unit)
n = 11	404	67	7.6	n = 11	315	35.9	10.3
n = 13	403.5	85	8.1	n = 13	325	43.1	10.1
n = 15	403	100	8.3	n = 15	330	47.0	9.5
n = 17	403	120	8.8	n = 17	338	55.8	9.7

in Figure 4 (see also Supporting Information). The compound is zinc stearate. There are no absorption bands in the 3000−3500-cm^{-1} region, indicating the absence of water of hydration in the zinc soaps. This was also confirmed by thermogravimetry analysis (TGA) measurements (see Supporting Information). The C−H stretching modes of the methyl and methylene groups of the alkyl chains appear between 2800 and 3000 cm^{-1}. The two intense bands at 2848 and 2916 cm^{-1} are assigned to the symmetric ($\nu_s(CH_2)$), d^+) and the antisymmetric ($\nu_{as}(CH_2)$, d^-) stretching vibration of methylene groups. The peak at 2954 cm^{-1} is assigned to the antisymmetric ($\nu_{as}(CH_3)$, r$^-$) stretching vibration of the terminal methyl group; the methyl symmetric stretching mode expected at 2871 cm^{-1} is not seen. It is well known that the methylene stretching mode frequencies are sensitive to the conformation of the alkyl chain shifting to higher frequencies with increased conformational disorder.[15] The position of the methylene stretching modes for the zinc soaps, 2848 and 2916 cm^{-1}, indicates that the alkyl chains are essentially in an all-trans conformation.[16,17]

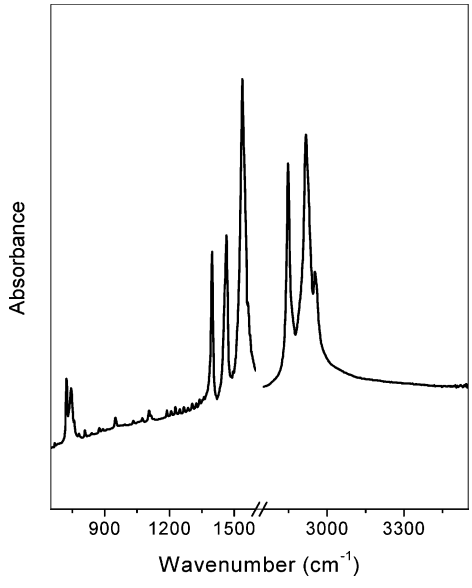

Figure 4. Room-temperature infrared spectra of zinc stearate.

The peak at 719 cm^{-1} is assigned to the CH_2 rocking vibration. The fact that this band as well as CH_2 scissoring mode at 1467 cm^{-1} appear as a singlet implies hexagonal subcell packing.[18] These bands are known to split into two distinct components as a results of crystal or factor-group splitting in hexagonal or monoclinic packing.[19] The weak bands appearing between 1350 and 750 cm^{-1} are the progression bands arising from the coupling of the scissoring, wagging, and twisting modes of the methylene group and are discussed in detail in a subsequent section.

In the region below 1650 cm^{-1} the two intense peaks at 1398 and 1540 cm^{-1} are assigned to the symmetric ($\nu_s(COO)$) and antisymmetric ($\nu_{as}(COO)$) stretching modes, respectively, of the carboxylate group.[20] The difference in the positions of the carboxylate antisymmetric stretching and the symmetric stretching modes is indicative of the nature of metal−carboxylate coordination. The observed difference of 142 cm^{-1} in the zinc soaps is characteristic of bridging bidentate coordination.[21] This difference in frequencies is the same in all four compounds, indicating that there is no change in the nature of zinc−carboxylate coordination with chain length.

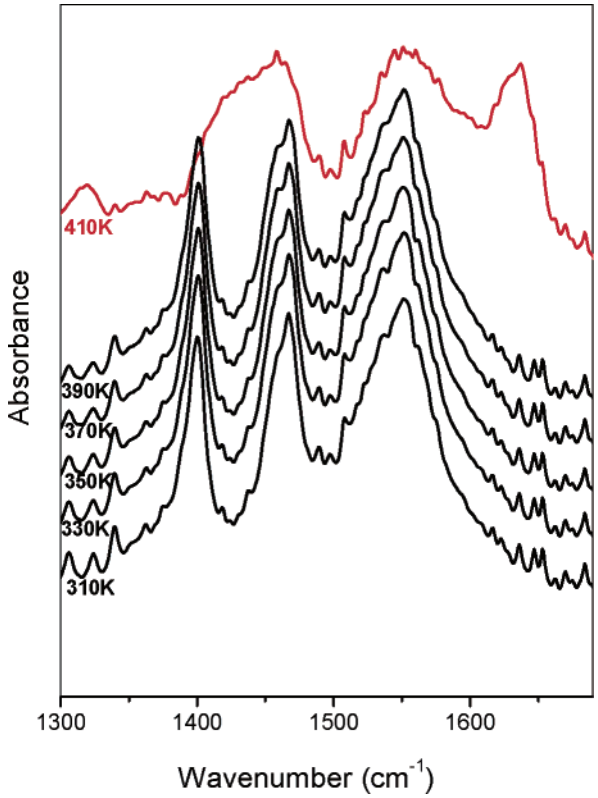

Figure 5. Infrared spectrum of zinc stearate in the carboxylate stretching region at different temperatures. The spectrum above melting is shown in red.

With increase in temperature changes in conformation of the alkyl chains as well as in the nature of the carboxylate−zinc coordination occur. The latter is reflected in the changes in the carboxylate stretching modes with temperature (Figure 5). The most significant changes in this region of the spectra occur at the melt. At the phase transition (melting), the symmetric stretching band ν_s(COO) becomes very broad and shifts to higher frequencies, 1424 cm^{-1}, merging with the CH_2 scissoring mode at the 1467-cm^{-1} band. The antisymmetric ν_{as}(COO) band also shifts to a higher frequency and is split into two bands at 1544 and 1634 cm^{-1}. The peak at 1634 cm^{-1} is a new feature. It is well established that the magnitude of $\Delta\nu$, the separation between ν_{as}(COO) and ν_s(COO) frequencies, may be used to distinguish between monodentate, bridging bidentate, and chelating bidentate modes of carboxylate coordination to the metal.[21] At melt the difference in frequencies $\Delta\nu$ between the antisymmetric and symmetric modes (1544−1424 cm^{-1}) are 120 and 210 cm^{-1} (1634−1424 cm^{-1}). The former is characteristic of bridging bidentate, while a difference of 210 cm^{-1} indicates monodentate coordination. These results are similar to those reported earlier for divalent metal carboxylates.[22] In the melt there is, therefore, a mixture of both bridging as well as monodentate zinc−carboxylate coordination. It is this change in coordination that results in the breaking up of the layer at the melting temperature. It may be noted that the change in carboxylate coordination occurs abruptly at melt.

Increase in temperature also induces changes in alkyl chain conformation. The methylene stretching modes that are sensitive to chain conformation shift gradually with temperature to higher frequencies. The symmetric and antisymmetric methylene stretching modes that appear at 2846 and 2916 cm^{-1}, respectively, at room temperature shift progressively to higher wavenumbers and just above the melt appear at 2854 and 2925 cm^{-1}, respectively (see Supporting information). These values are typical of alkyl chains having a large concentration of gauche

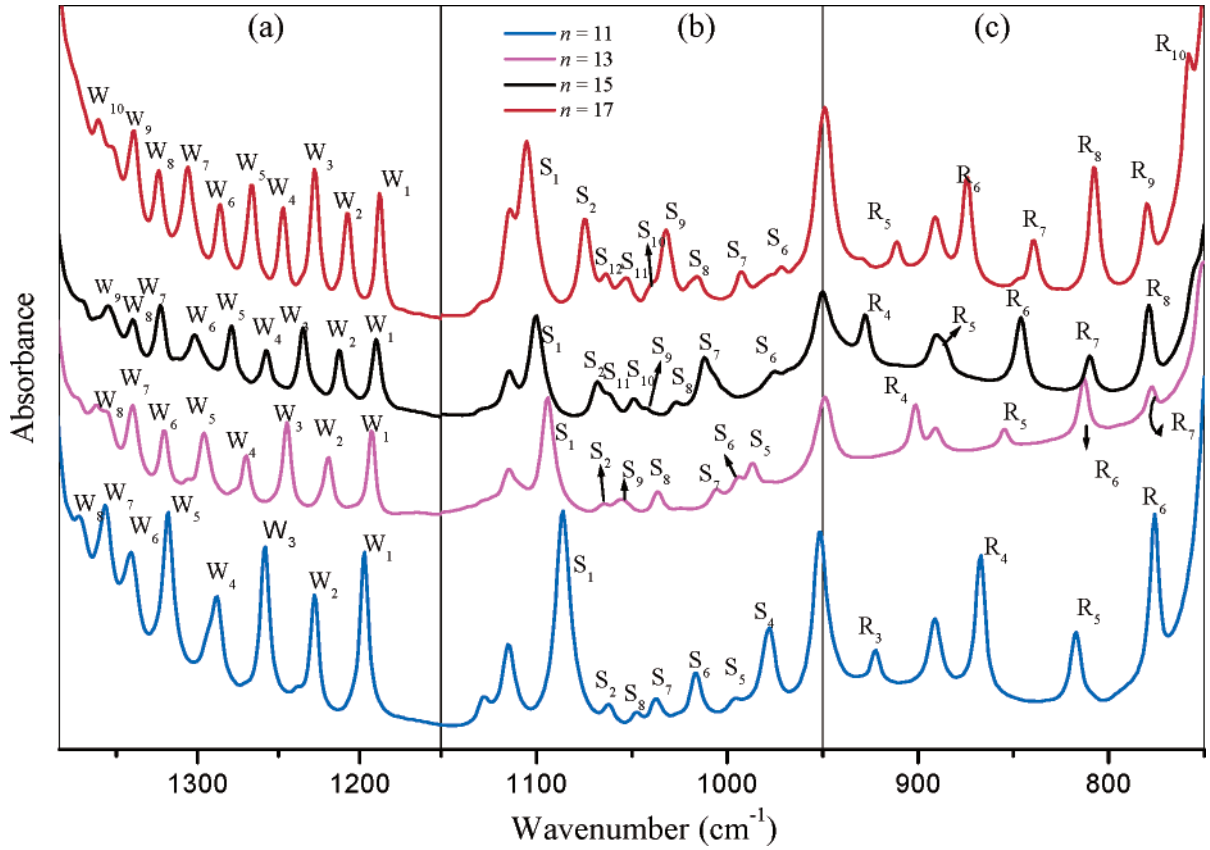

Figure 6. Infrared spectra in (a) the wagging (W_k), (b) the stretching (S_k), and (c) rocking (R_k) band progression regions of $Zn(C_nH_{2n+1}COO)_2$; n =11, 13, 15, 17. Bands are labeled by their k value.

TABLE 2: Observed Peak Positions of Methylene Wagging and Rocking-twisting Band Progressions in the $Zn(C_nH_{2n+1}COO)_2$

n = 17		n = 15		n = 13		n = 11	
ν (cm^{-1})	assignment	ν (cm^{-1})	assignment	ν (cm^{-1})	assignment	ν (cm^{-1})	assignment
1360	W_{10}	1353	W_9	1354	W_8	1356	W_7
1339	W_9	1338	W_8	1339	W_7	1340	W_6
1324	W_8	1323	W_7	1320	W_6	1318	W_5
1306	W_7	1300	W_6	1296	W_5	1289	W_4
1286	W_6	1279	W_5	1269	W_3	1258	W_4
1266	W_5	1257	W_4	1244	W_3	1327	W_2
1247	W_4	1235	W_3	1218	W_2	1196	W_1
1228	W_3	1213	W_2	1194	W_1	1086	S_1
1208	W_2	1190	W_1	1094	S_1	1061	S_2
1188	W_1	1100	S_1	1066	S_2	1046	S_8
1105	S_1	1068	S_2	1055	S_9	1037	S_7
1075	S_2	1061	S_{11}	1037	S_8	1017	S_6
1063	S_{12}	1049	S_{10}	1006	S_7	995	S_5
1053	S_{11}	1042	S_9	995	S_6	977	S_5
1041	S_{10}	1027	S_8	987	S_5	R_3	921
1032	S_9	1012	S_7	901	R_4	R_4	865
1016	S_8	975	S_6	855	R_5	R_5	816
990	S_7	928	R_4	814	R_6	R_6	776
970	S_6	886	R_5	778	R_7	R_{7-10}	720
911	R_5	846	R_6	720	R_{8-12}		
874	R_6	810	R_7				
840	R_7	779	R_8				
808	R_8	767	R_9				
780	R_9	720	R_{10-14}				
758	R_{10}						
720	R_{11-16}						

disorder like in the alkane melt.[16] Although the methylene stretching modes are sensitive to chain conformation, it is not possible to obtain quantitative information on the extent of conformational disorder from the position of these modes. This information may, however, be obtained from an analysis of the progression bands in the infrared spectrum, described in the subsequent section.

Infrared Progression Bands. Vibrational spectra of long alkyl chain molecules have been interpreted on the basis of vibrational modes of an infinite polymethylene chain.[23,24] Conformational order causes a coupling of the vibrational modes of methylene units in the trans registry giving rise to a series of progression bands in the infrared. These modes are delocalized over the length of the all-trans segment, and their spacing and position depend on the number of coupled trans CH_2 units and hence can provide a quantitative measure of chain conformation. Vibrational modes in an all-trans methylene chain are described through a coupled oscillator model for which the eigenvalues are given by[25]

$$4\pi^2\nu^2 = H_0 + 2\Sigma H_m(\cos m\varphi_k)$$

where H_0 and H_m are the matrix elements of the secular determinant. φ is the phase difference between adjacent oscillators as given by

$$\phi_k = k\pi/(N+1), (k = 1,2,..,N)$$

where N is the number of coupled oscillators or as in the present, coupled *trans*-CH_2 units. For an infinite polymethylene chain only vibrational modes at $\varphi = 0$ or π are infrared and/or Raman allowed. For a finite chain, however, in addition to the $\varphi = 0$ or π modes, a series of bands, namely, progression bands, appear in the vibrational spectrum. The progression bands appearing in the spectrum are analyzed by assigning a k value after identifying the particular mode to which it belongs. When correctly assigned a smooth curve results from a plot of ν_k vs ϕ_k.

The progression bands arising from the coupling of CH_2 wagging (ν_3), twisting-rocking (ν_7), rocking-twisting (ν_8), and C−C skeletal stretch (ν_4) modes have been studied in detail for *n*-alkanes,[26] *n*-alchols,[27] fatty acids,[28] and surfactants intercalated in layered solids.[29,30]

The progression bands in the infrared spectrum of $Zn(C_nH_{2n+1}COO)_2$; n =11, 13, 15, 17 are shown in Figure 6. The bands in the 1400−1150-cm^{-1} region arise from the wagging (ν_3,W_k) progression bands; the C−C stretching (ν_4,S_k) progres-

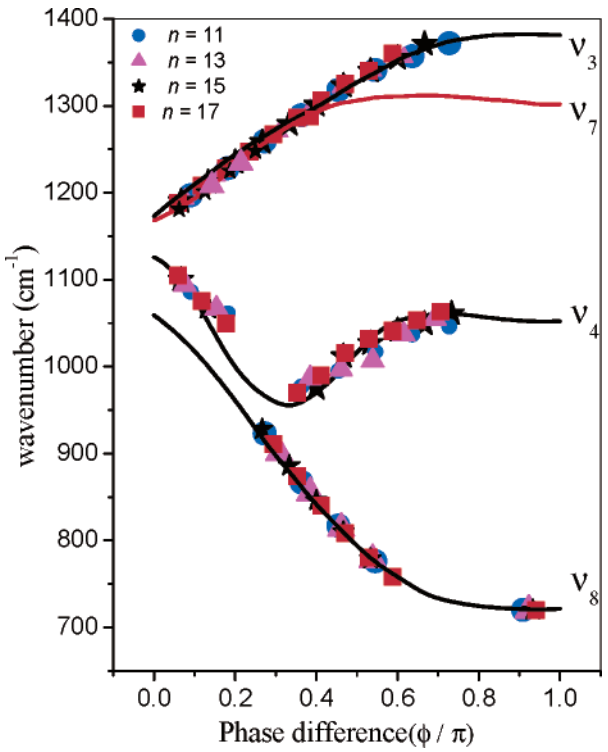

Figure 7. Dispersion of the progression bands of of $Zn(C_nH_{2n+1}COO)_2$; n =11, 13, 15, 17. The solid line is the calculated dispersion curve for an infinite polymethylene chain.[31,32]

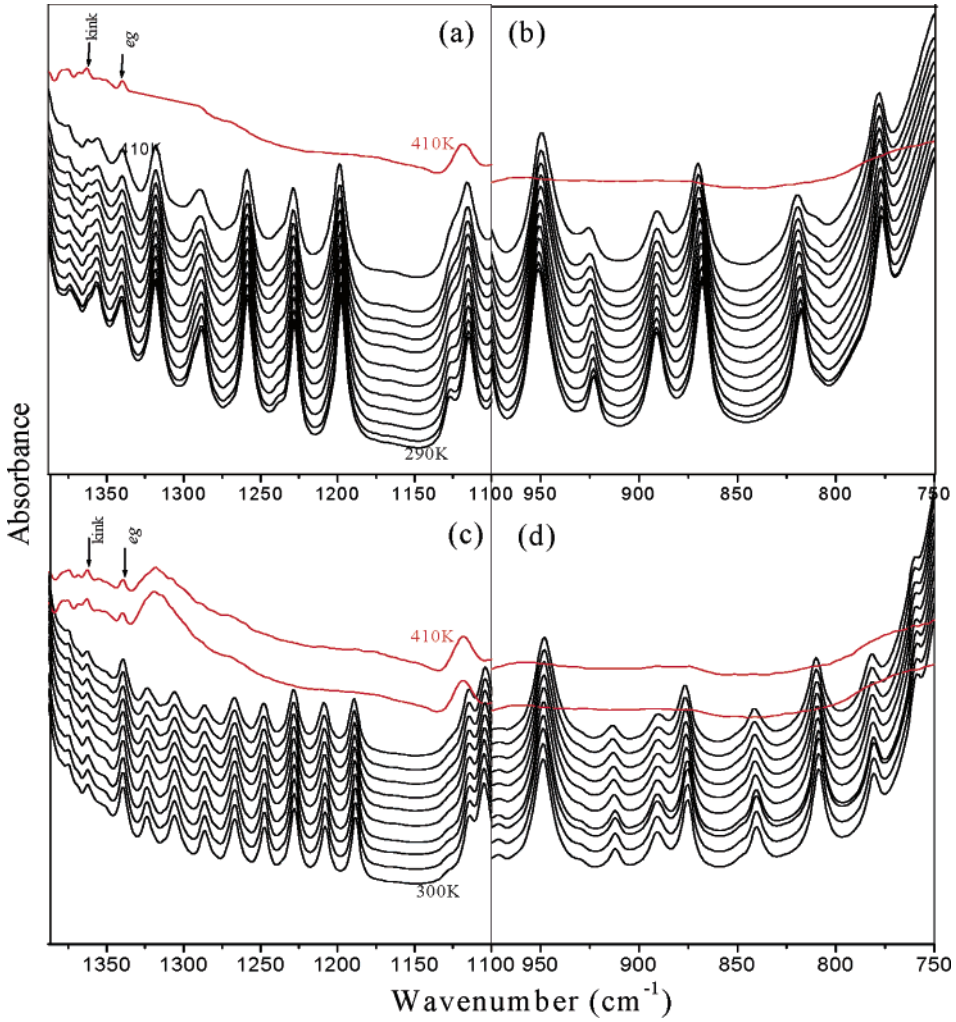

Figure 8. Infrared spectra in the wagging (1400−1100 cm^{-1}) and rocking (100−750 cm^{-1}) progression band regions of zinc stearte (a and b) and zinc lauriate (c and d) at different temperatures. Spectra have been recorded at 10 K intervals. Spectra above melt are shown in red.

sion bands appear between 1150 and 950 cm^{-1}, while the CH_2 rocking (R_k) modes appear between the 1000- and 700-cm^{-1} region of the infrared spectrum. The twisting modes that appear as weak shoulders to the wagging modes are not clearly seen in the zinc soaps. It may be seen from Figure 6 that as the alkyl chain length increases the number of progression bands increase with a corresponding decrease in the interband separation. For all four compounds, k values could be assigned to the bands in the progression series assuming that all methylene units in the alkyl chain are in trans registry or in other words the number of coupled oscillators, N, in the $Zn(C_nH_{2n+1}COO)_2$ compounds has a value of $(n - 1)$. The positions and assignments of the progression bands are provided in Table 2 and also indicated in Figure 6. The observed band positions have been plotted as a function of the phase difference, ϕ_k, in Figure 7. It may be seen that, for a particular mode, all points lie on an identical curve irrespective of the chain length. The experimental dispersion, in fact, lies on the calculated dispersion curve for an infinite polymethylene chain.[31,32] The fact that all experimental points lie on a smooth dispersion curve validates the assignment of k values in Figure 6 that, in turn, justifies the assumption that in the zinc soaps all methylene units irrespective of chain length are in trans registry. These results unequivocally establish that in the $Zn(C_nH_{2n+1}COO)_2$ soaps the alkyl chains adopt an all-trans planar conformation and that the progression bands in Figure 6 provide a characteristic signature of all-trans chains in these compounds.

Increase in temperature induces conformational disorder in the methylene chains. Chains having one or more gauche defects will no longer contribute to the intensity of the progression bands that are associated with the all-trans alkyl chains. The intensities of these bands are, therefore, directly proportional to the concentration of all-trans chains. If the gauche defects appear at different locations in different chains the length of the all-trans segments in each chain would be different. The intensities of the progression bands associated with these all-trans segments would be too small to be observed, and no additional progression series would be seen with increase in temperature. The infrared spectra at different temperatures in the wagging (1400−1100 cm^{-1}) and rocking (1050−750 cm^{-1}) band progression series of zinc stearate (N =16) and zinc lauriate (N=10) are shown in Figure 8. It may be seen in that in both compounds the melt is characterized by the abrupt disappearance of progression band intensity and the appearance of features due to specific conformational defect sequences[33] end gauche at 1342 cm^{-1} and kink (gauche−trans−gauche) at 1365 cm^{-1}. The melt is therefore characterized by the total absence of all-trans chains.

The progression band intensities of Figure 8 provide a quantitative measure of methylene chain conformation, since only methylene chains with an all-trans conformation contribute to the progression band intensities. By assumption that at room temperature all alkyl chains are ordered in an all-trans conformation, then the ratio of the intensities of the progression bands at any temperature with respect to the intensity at room

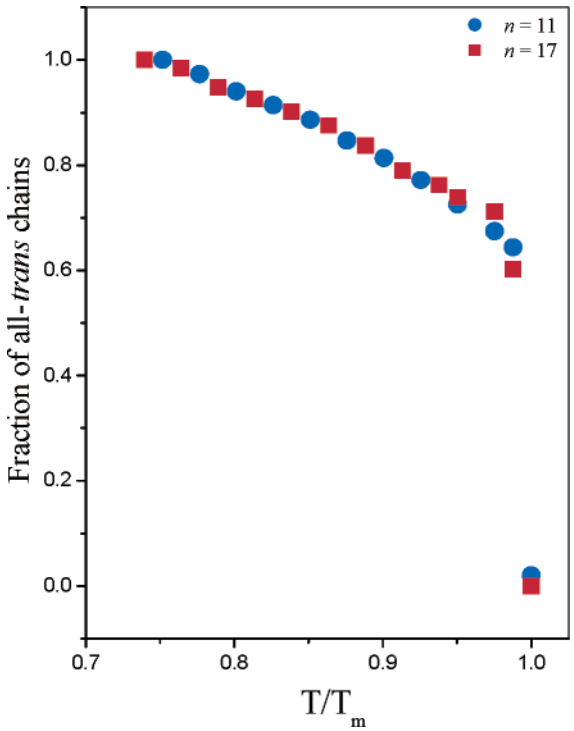

Figure 9. Fraction of all-trans methylene chains in zinc stearate and zinc lauriate at different temperatures. T_m is the melting temperature, 403 K.

temperature would be directly proportional to the fraction of alkyl chains in the zinc soaps that have an all-trans conformation at that temperature.[34] The intensity at different temperatures was obtained by summing up the progression band intensities for both wagging and rocking modes for all values of *k* associated with that series. The variation of the ratio of the intensity of the progression bands at different temperatures with respect to that at room temperature for zinc stearate and zinc lauriate is shown in Figure 9. It may be seen that for both the compounds the variation of the ratio is identical and melting occurs when ~30% of the alkyl chains are disordered and that the thermal evolution of conformational disorder is similar for zinc stearate and zinc lauriate, the longest and shortest fatty acid zinc soaps investigated in the present study. These results highlight the universal nature of the melting phase transition in the saturated fatty acid zinc soaps.

A conformationally disordered chain requires a larger lateral area as compared to an all-trans chain. Since fatty acid chains in the soaps are coordinated to the zinc layer, there is critical concentration of disordered chains that the layer can sustain. Above this concentration the carboxylate−zinc coordination is forced to change from being purely bridging bidentate to a mixture of mono- and bidentate coordination with the consequent breaking up of the layer. This breakup results in the melting of the solid as confirmed by disappearance of all Bragg reflections in the powder X-ray patterns at this temperature. The structure of the zinc layer and the nature of coordination are the same irrespective of the chain length; it is, therefore, natural that the critical concentration (~30%) of disordered chains at which melting occurs would be identical and since the thermal evolution of disorder, too, is similar the melting temperature of the zinc soaps the same.

Conclusions

The melting of alkyl chains in the saturated fatty acid zinc soaps of different chain lengths, $Zn(C_nH_{2n+1}COO)_2$; $n = 11$, 13, 15, and 17, have been investigated by powder X-ray diffraction, DSC, and vibrational spectroscopy. These soaps pass directly from the solid to the liquid phase without any intermediate mesophases making them one of the simpler model systems for studying the melting phenomena. The present study highlights the universal nature of the melting transition in these compounds. $Zn(C_nH_{2n+1}COO)_2$ has a layer structure with alkyl chains arranged as tilted bilayers with all methylene chains adopting a planar, all-trans conformation at room temperature. This was established from X-ray diffraction and the progression bands in the infrared spectra. The progression bands arise from the coupling of vibrational modes of all-trans methylene units and the assignments of these bands in the zinc soaps indicates that in $Zn(C_nH_{2n+1}COO)_2$ all $(n - 1)$ methylene units are in trans registry.

All four compounds, $Zn(C_nH_{2n+1}COO)_2$, show a single reversible melting phase transition in the DSC. An interesting feature of the melting transition in these zinc soaps is that although the enthalpy change shows a linear variation with alkyl chain length the melting temperature shows no change and is 403 K for all values of *n*. Melting is associated with the conformational disordering of the chains as well as a change in the zinc−carboxylate coordination from bridging bidentate to a mixture of bridging bidentate and monodentate coordination. Whereas conformational changes occur gradually with increase in temperature, the change in carboxylate−zinc coordination occurs abruptly at melt resulting in the layers breaking up and the melting of the solid. The progression bands are a characteristic signature of all-trans chains and the variation of their intensities with temperature provide a quantitative measure of the fraction of all-trans chains present in the soap at different temperatures. It is observed that, irrespective of chain length, melting of saturated fatty acid zinc soaps occur when 30% of the chains are disordered (having one or more gauche bonds). This is understandable since alkyl chains irrespective of chain length are attached to the zinc layer in an identical fashion the critical concentration of disordered chains at which melting occurs, too, would be identical. These results provide a simple explanation for the universal nature of the melting transition observed in the saturated fatty acid zinc soaps.

Supporting Information Available: TGA of zinc stearate. Infrared spectrum of zinc stearate zinc palmitate, zinc myristate, and zinc lauriate and the table of observed band positions and assignments in the infrared spectrum of the zinc stearate. Powder X-ray diffraction patterns of zinc stearate at different temperatures and the corresponding interlayer spacing vs temperature. Infrared spectra of zinc stearate in the C−H stretching region at different temperatures.

References and Notes

(1) Ishioka, T.; Wakisaka, H.; Saito, T. and Kanesaka, I. *J. Phys. Chem. B* **1998**, *102*, 5239.
(2) Bracconi, P.; Andrès, C.; Ndiaye, A. *Int. J. Pharm.* **2003**, *262*, 109.
(3) Akanni, M. S.; Okoh, E. K.; Burrows, H. D.; Ellis, H. A. *Thermochim. Acta* **1992**, *208*, 1−41.
(4) Bossert, R. G. *J. Chem. Educ.* **1950**, *63*, 221.
(5) Konkoly-Thenge, I.; Ruff, I.; Andeosun, S. O.; Sime, S. J. *Thermochim. Acta* **1978**, *24*, 89.
(6) Ferloni, P.; Westrum, E. F. *J. Pure Appl. Chem.* **1992**, *64*, 73−78.
(7) Nishino, Y.; Yano, S.; Tansho M.; Yamaguchi, T. *Chem. Phys. Lett.* **1998**, *296*, 408.
(8) Gavrilko, T.; Drozdb, M.; Puchkovskaya, G.; Naumovets, A.; Tkachenko, Z.; Viduta, L.; Baran, J.; Ratajczak, H. *J. Mol. Struct.* **1998**, *450*, 135−139.
(9) Li. H.; Bu. W.; Wu, L. *J. Phys. Chem. B* **2005**, *109*, 21669.
(10) Binnemans, K.; Jongen, L.; Bromant, C.; Hinz, D.; Meyer, G. *Inorg. Chem.* **2000**, *39*, 5938.

(11) Ishioka, T.; Maeda, K.; Watanabe, I.; Kawauchi, S.; Harada, M. *Spectrochim. Acta A* **2000**, *56*, 1731.
(12) Barman, S.; Vasudevan, S. *J. Phys. Chem. B* **2006**, *110*, 651
(13) Lacouture, F.; Peultier, J.; Francois, M.; Steinmetz, J. *Acta Cryst.* **2000**, *C56*, 556
(14) Seuriun, P.; Guillon, D.; Skoulios, A. *Mol. Cryst. Liq. Cryst.* **1981**, *65*, 85.
(15) Snyder, R. G.; Strauss, H. L.; Elliger, C. A. *J. Phys. Chem.* **1982**, *86*, 5145.
(16) MacPhail, R. A.; Strauss, H. L.; Snyder, R. G.; Elliger, C. A. *J. Phys. Chem.* **1984**, *88*, 334.
(17) Zerbi, G.; Del Zoppo, M. in *Modern Polymer Spectroscopy*; Zerbi, G., Ed.; Wiley-VCH: Germany 1999.
(18) Snyder, R. G. *J. Mol. Spectrosc*. **1961**, *7*, 116.
(19) Uno, T.; Machida, K.; Miyajima, K. *Spectrochim. Acta* **1968**, *24A*, 1749.
(20) Nakanato, K.; McCarthy, P. J. *Spectroscopy and Structure of Metal Chelate Compounds*; John Wiley: New York, 1968; p 268
(21) Acock, N. W.; Tracy, V. M.; Waddington, T. C. *J. Chem. Soc., Dalton Trans.* **1976**, 2243.
(22) Mesubi, M. A. *J. Mol. Struct.* **1982**, *81*, 61.
(23) Tasumi, M.; Shimanouchi, T.; Miyazawa, Y. *J. Mol. Spectrosc.* **1962**, *9*, 261.
(24) Schachtschneider, J. H.; Snyder, R. G. *Spectrochim. Acta* **1963**, *19*, 117.
(25) Snyder, R. G. *J. Mol. Spectrosc.* **1960**, *4*, 411.
(26) Snyder, R. G.; Schachtschnelder, J. H. *Spectrochim. Acta* **1963**, *19*, 85.
(27) Tasumi, M.; Shimaanouchi, T.; Watanabe, A.; Goto, R. *Spectrochim. Acta* **1964**, *20*, 629.
(28) Kobayashi, M.; Kaneko, F.; Sato, K.; Suzuki, M. *J. Phys. Chem.* **1989**, *93*, 485.
(29) Venkataraman, N. V.; Vasudevan, S. *J. Phys. Chem. B* **2001**, *105*, 7639.
(30) Venkataraman, N. V.; Vasudevan, S. *J. Phys. Chem. B* **2002**, *106*, 7766−7773
(31) Tasumi, M.; Shimanouchi, T.; Miyazawa, Y. *J. Mol. Spectrosc.* **1962**, *9*, 261.
(32) Schachtschneider, J. H.; Snyder, R. G. *Spectrochim. Acta* **1963**, *19*, 117.
(33) Snyder, R. G. *J. Chem. Phys.* **1967**, *47*, 1316.
(34) Venkataraman, N. V.; Vasudevan, S. *J. Phys. Chem. B* **2003**, *117*, 10119.